Friction stir welding characteristics of 2017-T351 aluminum alloy sheet

H. J. LIU*
National Key Laboratory of Advanced Welding Production Technology, Harbin Institute of Technology, Harbin 150001, People's Republic of China
E-mail: liuhj@hope.hit.edu.cn

H. FUJII, K. NOGI
Joining and Welding Research Institute, Osaka University, Osaka 567-0047, Japan

Heat-treatable aluminum alloys are difficult to fusion weld because of easy formation of some welding defects such as crack and porosity in the weld [1]. Friction stir welding (FSW) is a solid state welding process in which the crack and porosity often associated with fusion welding processes are eliminated [1, 2]. Therefore, the FSW process is being studied to weld heat-treatable aluminum alloys in order to obtain high-quality joints [3–10]. However, some studies have indicated that FSW gives rise to the softening of heat-treatable aluminum alloys, thus resulting in the degradation of the mechanical properties of the joints. The degradation extent is related not only to the alloy type [9–11], but also to the alloy thickness [12–16]. 2017-T351 aluminum alloy is one of the 2xxx-series heat-treatable aluminum alloys, and a 5-mm thick 2017-T351 plate has been friction stir welded to examine the tensile properties and fraction locations of the joints [9]. This letter aims to further demonstrate the FSW characteristics of a 3-mm thick 2017-T351 sheet to comprehend the effect of alloy thickness.

The base material used in this study was a 3-mm thick 2017-T351 aluminum alloy sheet with the chemical compositions and mechanical properties listed in Table I. The sheet was cut and machined into rectangular welding samples, 300 mm long by 80 mm wide, and they were longitudinally butt-welded using an FSW machine. The designated welding tool size and welding parameters are listed in Table II, in which the revolutionary pitch (RP) is defined as the travel speed divided by the rotation speed. After welding, the joints were cross-sectioned perpendicular to the welding direction for metallographic analyses and tensile tests. The cross-sections of the metallographic specimens were polished with an alumina suspension, etched with Keller's reagent and observed by optical microscopy. The configuration and size of the transverse tensile specimens were prepared according to Fig. 1, in which RS and AS denote the retreating side and advancing side of the joint, respectively. Prior to the tensile tests, the Vickers hardness profiles across the weld nugget (WN), thermo-mechanically affected zone (TMAZ), heat affected zone (HAZ) and partial base material were measured along the centerlines of the cross-sections of the tensile specimens under a load of 0.98 N for 10 s, and the Vickers indentations with a spacing of 1 mm were also used to determine the fracture locations of the joints. The room temperature tensile tests were carried out at a crosshead speed of 1 mm/min, and the tensile properties of each joint were evaluated by three tensile specimens cut from the same joint.

Fig. 2 shows the tensile properties of the joints welded at different RP values. It can be seen from the figure that the tensile properties of each joint are all lower than those of the base material (see Table I), especially the elongation of the joint. When the RP is 0.07 mm/r, the maximum ultimate strength, 408 MPa, and elongation, 5.2%, are obtained, and such a strength is equivalent to 82% that of the base material. When the RP increases, the ultimate strength and elongation approximately decrease to 375 MPa and 3.1%, respectively, but the 0.2% proof strength slightly increases. These results indicate that a softening effect has occurred in the 3-mm thick 2017-T351 aluminum alloy sheet due to FSW just as it did in the 5-mm thick 2017-T351 plate, and the welding parameters affect the tensile properties of the 3-mm thick 2017-T351 joints, but such an effect is not as significant as that on the 5-mm thick 2017-T351 joints [9]. This implies that the greater the thickness of the aluminum alloy plate, the more significant the effect of the welding parameters. In other words, the range of welding parameters that can be used to weld a thinner 2017-T351 sheet is relatively wide.

Fig. 3 shows the fracture locations of the joints welded at different RP values. In this figure, the fracture location is expressed by the distance between the fracture surface and the weld center, and the distance is marked as a minus if the fracture occurs on the RS of the weld. It can be seen from Fig. 3 that the fracture locations of the joints are near the weld center although they change with RP. When the RP is smaller than 0.13 mm/r, the joints fracture within 0.5–0.6 mm of the weld center. When the RP is greater than 0.13 mm/r, the fracture occurs at the locations that are not more than 1.2 mm distant from the weld center. In addition, it should be noted that all the joints fracture on the RS of the weld. These results indicate that the welding parameters have a little effect on the fracture locations of the 3-mm thick 2017-T351 joints, and the RS is weaker than the AS of the weld. Such a situation is very different from

*Author to whom all correspondence should be addressed.

0022–2461 © *2005 Springer Science + Business Media, Inc.*

TABLE I Chemical compositions and mechanical properties of 2017-T351 aluminum alloy sheet

Chemical compositions (wt%)									Mechanical properties		
Al	Si	Fe	Cu	Mg	Mn	Ti	Zn	Cr	Ultimate strength	0.2% proof strength	Elongation
Bal.	0.52	0.29	4.29	0.60	0.58	0.02	0.08	0.02	495 MPa	327 MPa	20.1

TABLE II Tool size and welding process parameters used in the experiments

Tool size (mm)			Welding parameters			
Shoulder diameter	Pin diameter	Pin length	Tool tilt	Rotation speed	Travel speed	Revolutionary pitch
12	4	2.8	3°	1500 rpm	100–800 mm/min	0.07–0.53 mm/r

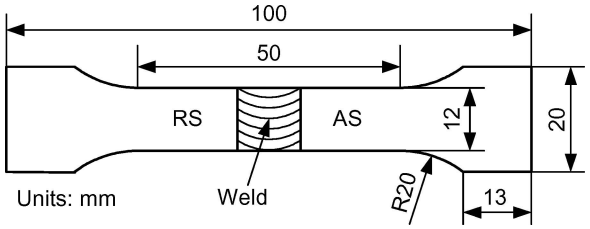

Figure 1 Configuration and size of the tensile specimens.

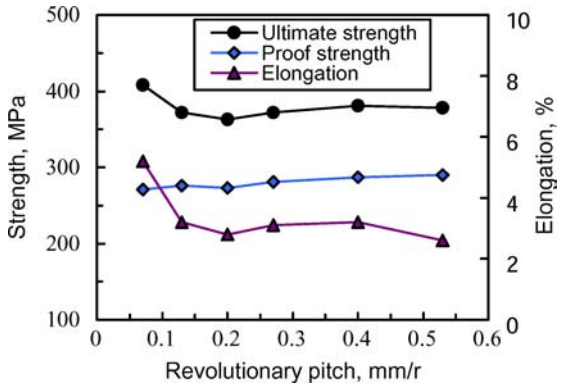

Figure 2 Tensile properties of the joints.

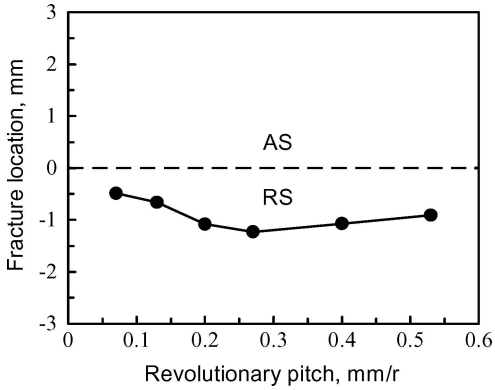

Figure 3 Fracture locations of the joints.

that observed in the 5-mm thick 2017-T351 joints [9]. This implies that the thickness of the aluminum alloy has an appreciable effect on the fracture locations of the joints. In detail, the joints for a thinner 2017-T351 sheet tend to fracture on the RS, while the joints for a thicker 2017-T351 plate are prone to fracture on the AS.

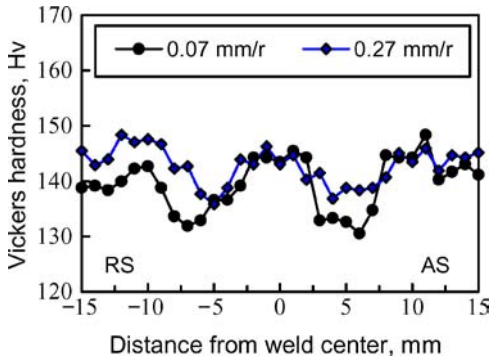

Figure 4 Microhardness profiles in the joints.

In most cases, the tensile properties and fracture locations of the joints are related to the hardness distributions in the joints [7–11]. Fig. 4 shows the microhardness profiles in the joints. It can be seen from this figure that a hardness degradation region, i.e. softened region, has occurred in the joints due to the effect of the FSW thermal cycle, thus the tensile properties of the joints are lower than those of the base material. When the RP increases, the minimum or average hardness in the joints increases, accordingly the 0.2% proof strength increases. However, the maximum ultimate strength and elongation are obtained only when the RP is relatively low (see Fig. 2), and the joints do not facture in the minimum-hardness zone (see Figs 2 and 3). This can be explained by the inner structures of the joints.

Fig. 5 shows the cross-sections and corresponding fracture locations of the joints. From the viewpoint of inner structures, a remarkable structural difference clearly exists between the WN and the TMAZ. The WN is composed of fine equiaxed recrystallized grains, while the TMAZ is composed of coarse-bent recovered grains. Therefore, the interface between the WN and the TMAZ is clearly visible and becomes a weaker region or location in the joint, and thus the joints are easy to fracture at this interface during the tensile testing although the hardness at this location is not a minimum. As shown in Fig. 5, the WN size is small no matter how much the RP changes, accordingly all the joints fracture near the weld center. In fact, the fracture in the joints is not only through the weaker interface between the WN and the TMAZ, but also through the stronger TMAZ above the WN (see Fig. 5c and d). Therefore, the tensile properties of the joints are dependent on both the

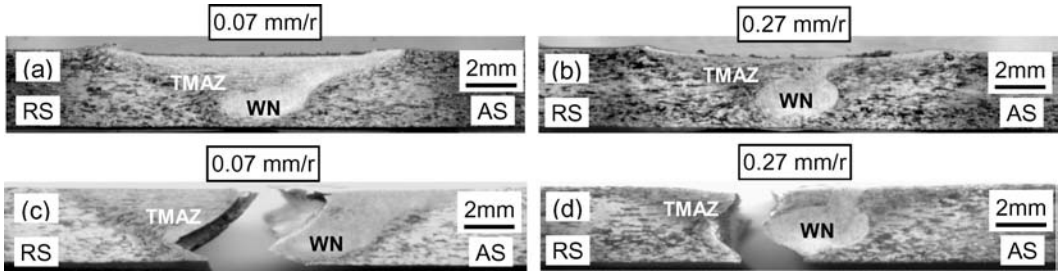

Figure 5 Photographs of the cross-sections and corresponding fracture locations of the joints: (a) and (b) cross-sections; (c) and (d) fracture locations.

interface and the TMAZ, and the smaller the vertical-direction interface of the elliptical WN, the higher the tensile properties of the joints. When the RP is lower, e.g. 0.07 mm/r, the vertical-direction interface between the WN and the TMAZ is smaller (see Fig. 5a), thus the tensile properties, including ultimate strength and elongation, are higher. On the other hand, when the RP is higher, e.g. 0.27 mm/r, the vertical-direction interface between the WN and the TMAZ is larger (see Fig. 5b), thus the ultimate strength and elongation are lower.

In summary, FSW clearly results in softening of the 3-mm thick 2017–T351 aluminum alloy sheet, thus the tensile properties of the joints are lower than those of the base material, and the maximum ultimate strength efficiency is 82%. The welding parameters do not significantly affect the tensile properties of the FSW joints, therefore the welding parameters for the 3-mm thick 2017-T351 aluminum alloy sheet can be varied over a relatively wide range. All the joints fracture near the weld center and on the RS of the weld. From the viewpoint of inner structures, the fracture locations of the joints occur at the interface between the WN and the TMAZ on the RS of the weld.

Acknowledgments

This work was performed at the Joining and Welding Research Institute (JWRI), Osaka University, Japan. Professor H. J. Liu would like to express his gratitude to JWRI for the financial support.

References

1. C. J. DAWES and W. M. THOMAS, *Weld. J.* **75** (1996) 41.
2. K. E. KNIPSTROM and B. PEKKARI, *ibid.* **76** (1997) 55.
3. M. G. DAWES, S. A. KARGER, T. L. DICKERSON and J. PRZYOATEK, in Proceedings of the 2nd International Symposium on Friction Stir Welding (Gothenburg, Sweden, June 2000) Paper No. S2-P1.
4. G. BUSSU and P. E. IRVING, in Proceedings of the 1st International Symposium on Friction Stir Welding (California, USA, June 1999) Paper No. S3–P1.
5. T. HASHIMOTO, S. JYOGAN, K. NAKADA, Y. G. KIM and M. USHIO, in Proceedings of the 1st International Symposium on Friction Stir Welding (California, USA, June 1999) Paper No. S9-P3.
6. M. KUMAGAI and S. TANAKA, in Proceedings of the 1st International Symposium on Friction Stir Welding (California, USA, June 1999) Paper No. S3-P2.
7. Y. S. SATO and H. KOKAWA, *Metall. Mater. Trans. A* **32** (2001) 3023.
8. M. W. MAHONEY, C. G. RHODES, J. G. FLINTOFF, R. A. SPURLING and W. H. BINGEL, *ibid.* **29** (1998) 1955.
9. H. J. LIU, H. FUJII, M. MAEDA and K. NOGI, *J. Mater. Process. Technol.* **142** (2003) 692.
10. *Idem*, *J. Mater. Sci. Lett.* **22** (2003) 1061.
11. *Idem*, *ibid.* **22** (2003) 441.
12. D. G. KINCHEN, Z. X. LI and G. P. ADAMS, in Proceedings of the 1st International Symposium on Friction Stir Welding (California, USA, June 1999) Paper No. S9-P2.
13. G. BIALLAS, R. BRAUN, C. D. DONNE, G. STANIEK and W. A. KAYSSER, in Proceedings of the 1st International Symposium on Friction Stir Welding (California, USA, June 1999) Paper No. S3-P3.
14. L. E. SVENSSON, L. KARLSSON, H. LARSSON, B. KARLSSON, M. FAZZINI and J. KARLSSON, *Sci. Technol. Weld. Join.* **5** (2000) 285.
15. H. J. LIU, H. FUJII, M. MAEDA and K. NOGI, *J. Mater. Sci. Lett.* **22** (2003) 41.
16. *Idem*, in Proceedings of the National Spring Meeting of JWS (Tokyo, Japan, 2003) p. 38.

Received 14 September
and accepted 8 November 2004